Ann. Geophysicae 18, 596–607 (2000) © EGS – Springer-Verlag 2000

Annales Geophysicae

# New model for auroral acceleration: O-shaped potential structure cooperating with waves

**P. Janhunen**[1], **A. Olsson**[1,2]

[1] Finnish Meteorological Institute, Geophysical Research, P.O. Box 503, FIN 00101 Helsinki, Finland
e-mail: Pekka.Janhunen@fmi.fi
[2] Swedish Institute of Space Physics, Uppsala Division, Uppsala, Sweden

Received: 27 May 1999 / Revised: 7 February 2000 / Accepted: 24 February 2000

**Abstract.** There are recent observational indications (lack of convergent electric field signatures above the auroral oval at 4 $R_E$ altitude) that the U-shaped potential drop model for auroral acceleration is not applicable in all cases. There is nevertheless much observational evidence favouring the U-shaped model at low altitudes, i.e., in the acceleration region and below. To resolve the puzzle we propose that there is a negative O-shaped potential well which is maintained by plasma waves pushing the electrons into the loss cone and up an electron potential energy hill at $\sim$3–4$R_E$ altitude range. We present a test particle simulation which shows that when the wave energization is modelled by random parallel boosts, introducing an O-shaped potential increases the precipitating energy flux because the electrons can stay in the resonant velocity range for a longer time if a downward electric field decelerates the electrons at the same time when waves accelerate them in the parallel direction. The lower part of the O-shaped potential well is essentially the same as in the U-shaped model. The electron energization comes from plasma waves in this model, but the final low-altitude fluxes are produced by electrostatic acceleration. Thus, the transfer of energy from waves to particles takes places in an "energization region", which is above the acceleration region. In the energization region the static electric field points downward while in the acceleration region it points upward. The model is compatible with the large body of low-altitude observations supporting the U-shaped model while explaining the new observations of the lack of electric field at high altitude.

**Key words:** Ionosphere (ionosphere-magnetosphere interactions; particle acceleration) – Magnetospheric physics (auroral phenomena)

*Correspondence to:* P. Janhunen

## 1 Introduction

Electron acceleration in discrete aurora is a long-standing question in space physics. A large body of observations below about 12 000 km altitude exists to support the U-shaped potential model (Carlqvist and Boström, 1970), see Bryant (1999) for a recent critical review. However, in a recent statistical study it was found that the convergent perpendicular electric field signatures which should be associated with the "upright legs" of the U-shaped potential are notably absent in Polar satellite data at about 4 $R_E$ altitude (Janhunen *et al.*, 1999). This casts some doubts on the applicability of the classical U-shaped model to describe auroral acceleration. By the classical U-shaped model we mean a potential geometry where the potential contours extend through the equatorial plane and close only in the opposite hemisphere.

When looking for alternative mechanisms, we can follow two lines of thought. First, the non-existence of convergent electric field led us to suggest that the potential geometry is O-shaped (Fig. 1) rather than U-shaped (Janhunen *et al.*, 1999). The idea is that above the usual acceleration region with upward parallel electric field at 1–2$R_E$ altitude there is another region of parallel electric fields at a higher altitude (presumably 2–4$R_E$) where the parallel electric field points downward. The second line of ideas of what might cause the acceleration, if not a potential drop, is wave-particle interaction, possibly lower-hybrid waves (Bryant *et al.*, 1991; Bingham *et al.*, 1988).

Concerning the U- and O-shaped potential models, a U-shaped potential drop accelerates electrons downward and ionospheric ions upward. An O-shaped potential barrier (a negative potential well) acts as a high-pass filter for electrons if wave-particle interactions are absent: low-energy electrons are reflected back while high-energy electrons get through without experiencing net acceleration. An O-shaped potential is expected to be a plasma cavity as well: ions move faster when they

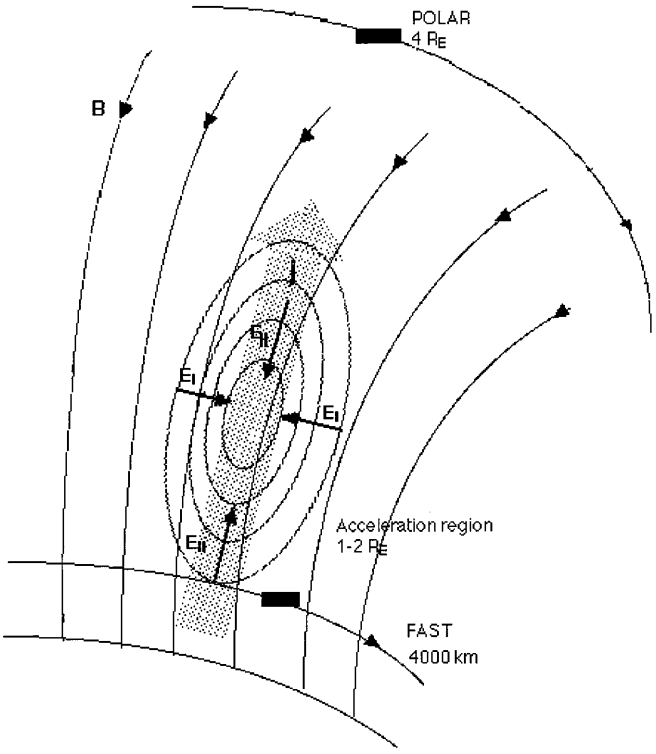


**Fig. 1.** The O-shaped potential model for auroral electric field. In the O-shaped potential model there need not be any strong electric fields at $4\,R_E$ Polar altitude from Earth's surface even though simultaneous low-altitude observations would show electrostatic shocks and parallel potential drops

are inside the structure and thus their density is reduced, while electrons are repelled by the structure so that their density is reduced for that reason. Being much larger than the Debye length, the O-shaped potential should be quasineutral.

An accelerated Maxwellian particle flux is given by

$$F(E) = \begin{cases} \dfrac{1}{\pi}\dfrac{n}{\sqrt{2\pi m_e}}\dfrac{E}{T^{3/2}}\mathrm{e}^{-\left(\frac{E-eV}{T}\right)}, & \text{if} \quad E > eV \\ 0, & \text{if} \quad E \le eV \end{cases} \tag{1}$$

where $n$ is the source plasma density, $T$ source plasma temperature in energy units, $E$ the particle energy and $eV$ the peak energy (Evans, 1974). Since this can also be written as

$$F(E) = \begin{cases} \dfrac{1}{\pi}\dfrac{n\mathrm{e}^{eV/T}}{\sqrt{2\pi m_e}}\dfrac{E}{T^{3/2}}\mathrm{e}^{-\frac{E}{T}}, & \text{if} \quad E > eV \\ 0, & \text{if} \quad E \le eV \end{cases} \tag{2}$$

it follows that we can interpret an inverted-V spectrum either as being accelerated by a potential drop $V$, which is the U-shaped interpretation, or as being the original source plasma distribution from which energies lower than $eV$ have been filtered out, which is the O-shaped interpretation. Thus the O-shaped potential can produce the same inverted-V spectra as the U-shaped potential, provided that the source plasma phase space density in the loss cone is large enough. The physical reason for this is that the lower half of an O-shaped potential *is* a U-shaped potential. Furthermore, because of this, much of the low-altitude phenomenology is the same in the U- and O-shaped models. For example, a satellite passing through the potential structure below the center of the "O" sees a convergent perpendicular electric field, and integrating the potential along the spacecraft orbit should produce the same result as the potential drop below the satellite (Marklund, 1993; McFadden *et al.*, 1998).

After looking at FAST/Polar conjunction events it has become clear to us that the phase space density observed at Polar at 4 $R_E$ altitude is in most cases too small to explain the conjugate FAST observations at low altitude in the O-shaped model. Thus the O-shaped model must be augmented by some nonadiabatic processes to bring it into quantitative correspondence with observations. In this work we will study the question by using a test-particle simulation model.

The study is structured such that in the Modeling section we describe the test-particle simulation, validate it by comparisons with analytic results, and apply it to two examples taken from satellite measurements. We then discuss the simulation results from a physical point of view and summarize the main findings from the simulation. Finally we present the new "cooperative" model for auroral acceleration, which is based on the simulation results.

## 2 Modeling

### *2.1 Model description*

To model the motion of auroral electrons in a given potential structure with a known source plasma distribution, we use a simple simulation program, which integrates the equations of conservation of total energy and the first adiabatic invariant in a dipolar magnetic field with a given potential structure. The lower boundary of the simulation box is set to the ionosphere ($s = 1.01725$) and the upper at $s = 5$. Here $s$ is the field-aligned coordinate in units of Earth radius. The wave-particle interaction part of the program is somewhat similar but unrelated to those presented earlier by Bryant and Perry (1995).

In the initialization stage the electrons are injected one at a time from the upper boundary. After the wanted number of particles have been injected, the number of particles in the system stays constant. Particles that are lost in the ionosphere reappear at the upper boundary with a random initial velocity. Mirrored electrons that exit through the upper boundary are also re-entered.

We will now describe the model that we have found to be the most appropriate for the purpose of reproducing inverted-V spectral peaks: At every time step (we use $\Delta t = 10$ ms), a fraction of particles at some altitude range (we use $2.5 \le s \le 4.25$) is given a parallel boost, such that the parallel kinetic energy is multiplied by a constant factor. The probability $P$ of giving a boost to a given electron is assumed to be $P = \min(1, \exp(-W_\parallel/\Delta W_{\mathrm{boost}}))$, where $W_\parallel$ is the original parallel

kinetic energy and $\Delta W_{\mathrm{boost}}$ is a given parameter, for example, $\Delta W_{\mathrm{boost}} = 200$ eV. Thus, low-energy electrons are boosted with a higher probability than higher energy ones. On the other hand, the absolute increase in parallel energy per boost is larger for higher energy electrons, because the original energy is multiplied by a constant factor. At each encounter the particle energy is multiplied by the factor $C_{\mathrm{boost}}$ which is equal to 2.5 or 5 depending on the case (see Table 1). Such a value for the energy increase per wave packet encounter could be physically speaking overestimated, but the net effect is determined also by how often the particles encounter the waves, which depends on the time step and on $\Delta W_{\mathrm{boost}}$ through the probability $P$. We prefer to use a higher value for $C_{\mathrm{boost}}$ and to repeat the process less frequently in order to speed up the calculation; in any case, $C_{\mathrm{boost}}$ gives information on the relative intensity of the waves. In this model, low-energy (a few hundred eV or less) particles undergo at least one boost with a high probability. Thus for low-energy particles, the wave packet set is "thick". Higher energy electrons, on the other hand, have an exponentially decreasing probability of being affected by waves.

This model simulates waves that have a parallel electric field component and whose parallel phase speed is in resonance with the parallel thermal speed of some of the electrons so that some of the electrons are accelerated by the waves in the parallel direction, i.e., they get a parallel boost. For the sake of generality, we assume both upward and downward-propagating waves to be present with equal weight. If the waves were known to be predominantly downward, it would make it even easier to reproduce inverted-V spectra.

In Table 1 we show the various parameters related to the O-shaped potential and the random parallel boosts for all runs. In all runs we used 60 000 particles and 10 ms time step. The duration of each run was 1 minute physical time. The model geometry is shown schematically in Fig. 2.

**Table 1.** Altitude of the center of the O-shaped potential, boost coefficient, minimum boost altitude, maximum boost altitude, and boost probability energy scale for the runs

| | $s_{\mathrm{O}}$ | $C_{\mathrm{boost}}$ | $s_{\mathrm{min}}^{\mathrm{boost}}$ | $s_{\mathrm{max}}^{\mathrm{boost}}$ | $\Delta W_{\mathrm{boost}}$ |
|---|---|---|---|---|---|
| SM/norand | – | 0 | – | – | – |
| SM | – | 0 | – | – | – |
| SMU | – | 0 | – | – | – |
| SMO | 2.5 | 0 | – | – | – |
| SMU/real | – | 0 | – | – | – |
| SMU/randboost | – | 2.5 | 2.5 | 4.25 | 100 eV |
| SMO/real | 2.5 | 0 | – | – | – |
| SMO/randboost | 2.5 | 2.5 | 2.5 | 4.25 | 100 eV |
| SM/randboost | – | 5 | 2.0 | 4.5 | 100 eV |
| MMU/real | – | 0 | – | – | – |
| MMU/randboost | – | 5 | 2.5 | 4.25 | 210 eV |
| MMO/real | 2.5 | 0 | – | – | – |
| MMO/randboost | 2.5 | 5 | 2.5 | 4.25 | 210 eV |
| MM/randboost | – | 5 | 2.5 | 4.25 | 210 eV |

Coding: SM, single-Maxwellian, MM, multiple-Maxwellian, U, U-shaped potential, O, O-shaped potential

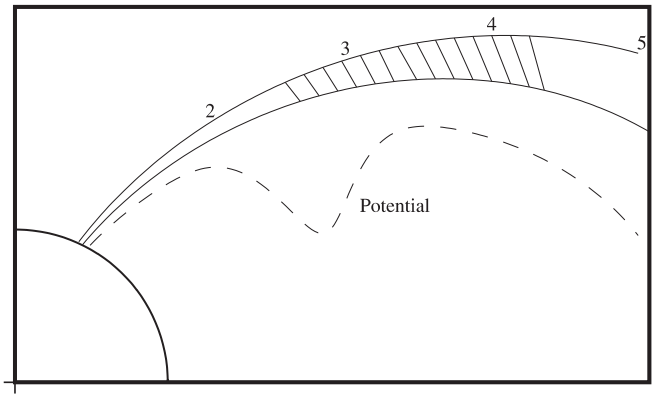


**Fig. 2.** Schematic picture of the SMO/randboost model geometry. An O-shaped potential whose central altitude is $s_{\mathrm{O}}$ is $2.5\,R_E$ and half-thickness $0.4\,R_E$ is indicated by *dashed line*. Random boosts are effective in the *hatched* altitude range. The $s$ values (field-aligned coordinate) are shown on *top*. Table 1 indicates how other models differ from this particular one

### 2.2 Validation

To validate the code, we first run it in cases where the resulting electron current density and electron energy flux into the ionosphere can be computed analytically.

First we run the program with no electric field and without random parallel boosts. In the first run we assume that particles that enter the simulation box again after exiting at the upper boundary do so without randomizing their velocity. This models a symmetric magnetic bottle with two ends (the southern hemisphere part of the system need not be simulated because of symmetry) with completely adiabatic electron motion. We use a single-Maxwellian initial plasma distribution and thus call the run SM/norand (Table 2). We expect the current density and energy flux to be zero or very small at the ionosphere after an initial transient phase, because all electrons that can precipitate do so during the first bounce and thereafter no particles enter the loss cone because the motion is completely adiabatic. The simulation gives these expected results (Table 2).

The second run SM is similar to SM/norand, except that now particle velocities are randomized at the upper boundary. This models a flux tube where some nonadiabatic mechanism operating above the upper boundary $s = 5$ randomizes the pitch angles completely during each electron bounce period, so that for downgoing electrons at $s = 5$, the loss cone is always filled. The result is shown in Fig. 3.

According to single-particle theory (Fridman and Lemaire, 1980), the electron current and energy flux at the ionospheric plane in the absence of potential structures are

$$j = en\sqrt{\frac{T}{2\pi m_e}} \tag{3}$$

$$\varepsilon = n\sqrt{\frac{T}{2\pi m_e}}2T \tag{4}$$

**Table 2.** Theoretically expected energy flux ($mW\,m^{-2}$), simulated energy flux, expected current density ($\mu A\ m^{-2}$), simulated current density, observed energy flux and observed current density for the runs. For validation runs, observed values are not applicable. Likewise, theoretical values are not given for runs containing non-adiabatic processes

| | $\varepsilon_{theo}$ | $\varepsilon_{sim}$ | $j_{theo}$ | $j_{sim}$ | $\varepsilon_{obs}$ | $j_{obs}$ |
|---|---|---|---|---|---|---|
| SM/norand | 0 | 0 | 0 | 0 | | |
| SM | 0.678 | 0.685 | 0.339 | 0.343 | | |
| SMU | 8.73 | 8.39 | 1.67 | 1.61 | | |
| SMO | 0.15 | 0.16 | 0.028 | 0.030 | | |
| SMU/real | 1.90 | 1.92 | 1.28 | 1.28 | 5.00 | 3.30 |
| SMU/randboost | | 2.82 | | 1.75 | 5.00 | 3.30 |
| SMO/real | 0.27 | 0.30 | 0.13 | 0.14 | 5.00 | 3.30 |
| SMO/randboost | | 2.31 | | 1.59 | 5.00 | 3.30 |
| SM/randboost | | 3.84 | | 1.97 | 5.00 | 3.30 |
| MMU/real | 4.03 | 4.21 | 0.59 | 0.61 | 6.37 | 1.07 |
| MMU/randboost | | 5.72 | | 0.79 | 6.37 | 1.07 |
| MMO/real | 1.14 | 1.27 | 0.11 | 0.12 | 6.37 | 1.07 |
| MMO/randboost | | 4.63 | | 0.73 | 6.37 | 1.07 |
| MM/randboost | | 2.69 | | 0.49 | 6.37 | 1.07 |

where a summation over all Maxwellian components of the source plasma is implicitly assumed (there is only one component in the SM case, however). $T$ is the source plasma temperature in energy units and $n$ is the number density. The theoretical values are shown in the first and third columns of Table 2 together with values given by the simulation. For run SM, these values are close together, showing agreement between simulation and theory.

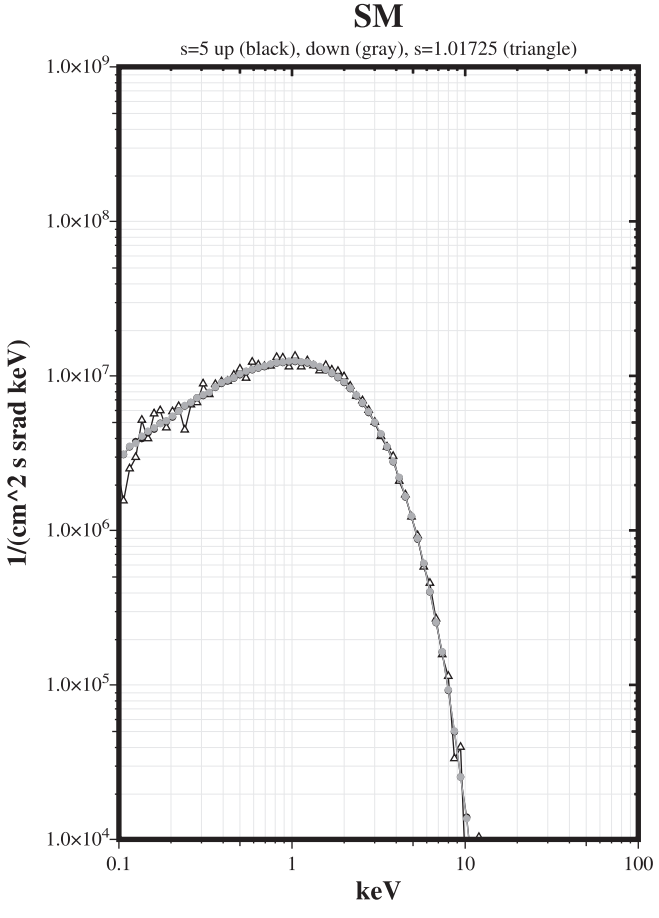


**Fig. 3.** SM: single-Maxwellian source plasma without potential structures or non-adiabatic processes. The *gray dots* show downgoing electron flux at the upper boundary, the *black dots* (which are mostly overlapped by the gray dots in this case) are the upgoing electrons at the upper boundary, and the *triangles* show the particle flux entering in the ionosphere at $s = 1.01725$. For low energies, some inaccuracy due to numerical noise can be seen

Next we include a U-shaped potential in the model (SMU). The analytical formulas are in this case (Fridman and Lemaire, 1980; Janhunen and Olsson, 1998)

$$j = e\left(\frac{B_i}{B_m}\right) n \sqrt{\frac{T}{2\pi m_e}} \left[1 - \frac{\exp(-xeV/T)}{1+x}\right] \tag{5}$$

$$\varepsilon = \left(\frac{B_i}{B_m}\right) n \sqrt{\frac{T}{2\pi m_e}} \left\{ 2T + eV - \mathrm{e}^{-xeV/T} \times \left[\frac{T + eV(1+x)}{1+x} + \frac{T + xT}{(1+x)^2}\right]\right\} \tag{6}$$

where $x = 1/(B_i/B_m - 1)$. Notice that Eq. (9) of Janhunen and Olsson (1998) contains an unfortunate printing error: the factor $T_\perp + eV(1 + x(T_\perp/T_\parallel))$ should be divided by $1 + x$. $B_i$ and $B_m$ are the magnetic fields at the ionosphere and at $s = 5$, respectively. The result of SMU is shown in Fig. 4. Again, we see from Table 2 that the simulation and theory are in agreement.

The next run is SMO, where we have a single-Maxwellian source plasma with an O-shaped potential (Fig. 5). The analytical formulas for the precipitating fluxes in an O-shaped potential are as follows:

$$j = en \sqrt{\frac{T}{2\pi m_e}} \frac{1}{b_o} \exp\left(\frac{-U}{T}\right) \times \left[b_i + (b_o - b_i)\exp\left(\frac{b_o U}{-b_i T + b_o T}\right)\right] \tag{7}$$

$$\varepsilon = n \frac{\mathrm{e}^{-U/T}}{b_o} \sqrt{\frac{T}{2\pi m_e}} \left[b_i(2T + U) + \mathrm{e}^{\frac{b_o U}{(b_o - b_i)T}}(2b_o T - b_i(2T + U))\right] . \tag{8}$$

The derivation of these formulas, which is straightforward in principle, will be published elsewhere. Here $b_o$ is the magnetic field at the center of the O-shaped potential. In the runs presented here, the center of the potential is put at $s = 2.5$. This formula is valid for a

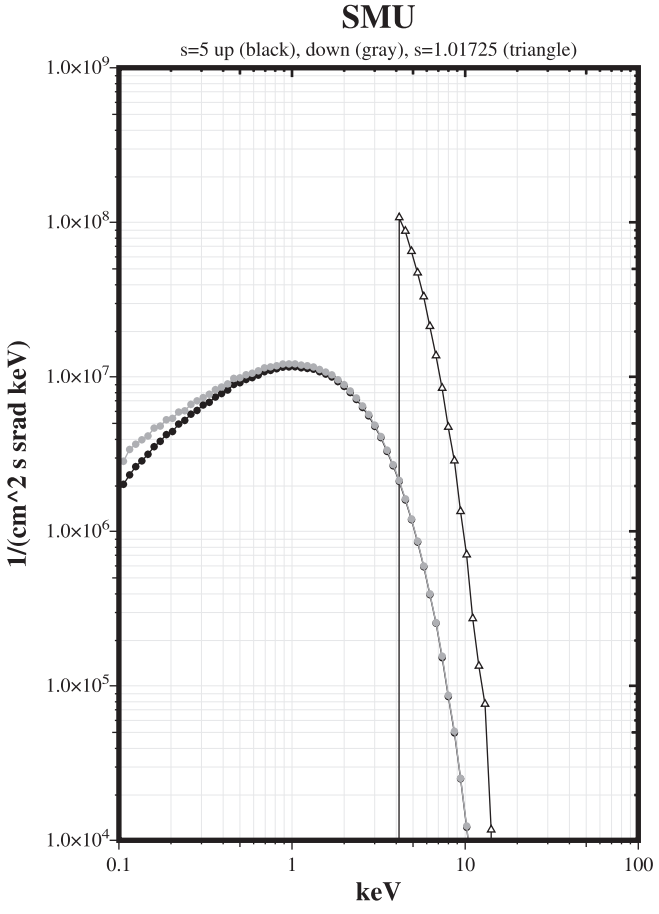


**Fig. 4.** SMU: single-Maxwellian source plasma and a U-shaped potential. This is the classical picture, where a potential drop accelerates the electrons

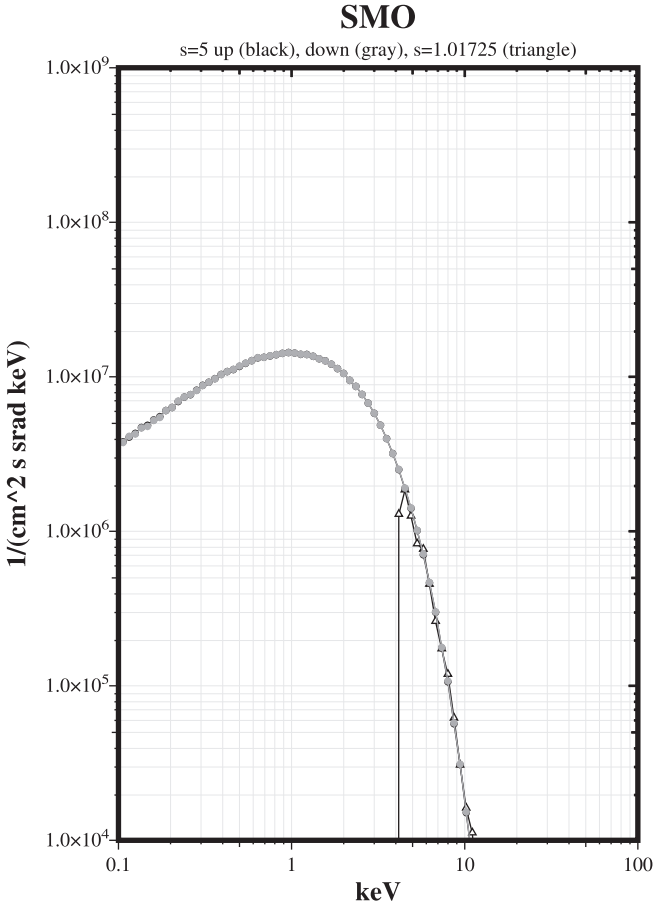


**Fig. 5.** SMO: single-Maxwellian source plasma and an O-shaped potential. Low-energy electrons are filtered out by the potential barrier and the high energy electrons retain their original flux. The precipitating flux is unrealistically low

thin potential barrier of depth $U$. From Fig. 5 we see that the electrons which have a lower energy than $U$ are filtered out before reaching the ionosphere, while other electrons get through and have their unmodified flux at the ionosphere. The small discrepancy with the simulated and expected energy flux in SMO (see Table 2) is due to the fact that the O-shaped potential in the model is represented by a Gaussian with half-thickness of $0.4\,R_E$ rather than an infinitely thin barrier. The potential is centered at the altitude given in Table 1. Comparing Figs. 4 and 5, one sees it clearly that the completely adiabatic O-shaped potential model produces too small ionospheric fluxes for the case at hand.

Thus we have shown that the program produces results that are in agreement with analytic formulas when adiabatic motion is assumed.

### *2.3 Reproduction of data*

We now turn away from validation and try to reproduce observed data from the simulation.

From a study of inverted-V auroral acceleration mechanisms using FAST/Polar satellite conjunctions which will be published elsewhere we have picked two typical FAST and HYDRA (Polar electron detector) conjunction electron spectra that we try to reproduce with our model. In one of the examples (Fig. 6), HYDRA shows a singly peaked non-plateau type electron spectrum, which we call "single-Maxwellian" (SM). In the other example (Fig. 7) the HYDRA spectrum has two peaks. We call such spectrum multiple-Maxwellian (MM). We have modeled the HYDRA spectra with two and three Maxwellians, respectively. The source plasma model parameters are given in the figures. Notice that we use 2 Maxwellians to model the "single-Maxwellian" case and 3 Maxwellians to model the "multiple-Maxwellian" case. The phrases "single-Maxwellian" (SM) and "multiple-Maxwellian" (MM) are only short mnemonic phrases we use to describe a differential particle flux spectrum which is "singly peaked and not containing a plateau" (SM) or "multiply peaked or plateau-containing" (MM).

In Fig. 8 we show the SMU/real run using the source plasma given in the caption of Fig. 6 and accelerate it by a U-shaped potential drop, whose magnitude is 1.01 kV which has been selected to match the peak position of FAST (Fig. 6). From Table 1 we see that the simulated energy flux is again in agreement with the theoretical prediction and is about 40% of the FAST-measured flux of 5 mW $m^{-2}$. More importantly, the simulated peak is

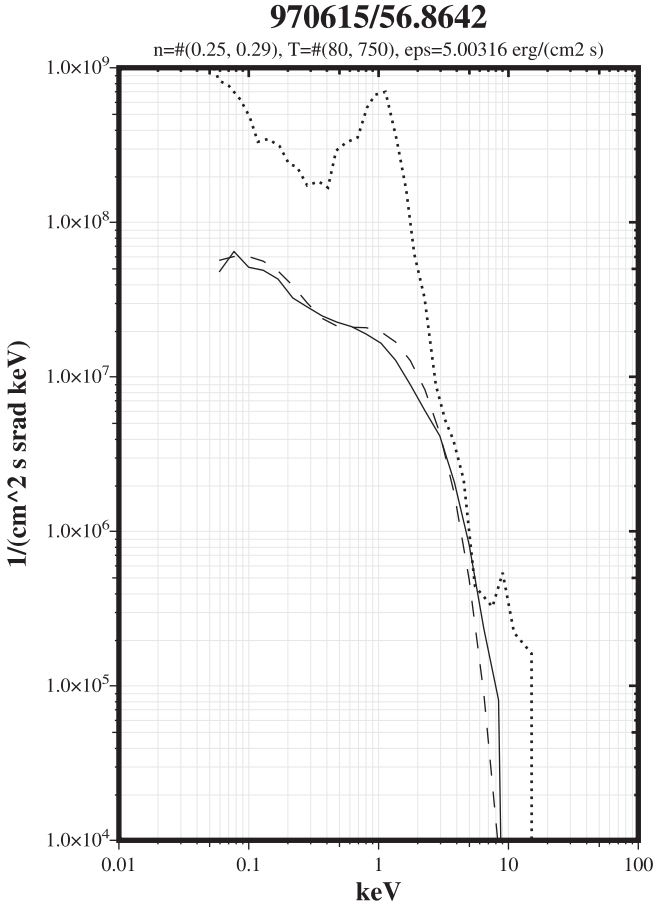


**Fig. 6.** The single-Maxwellian data example. The *dotted line* is the measured FAST electron flux. The particles on the *left* of the *peak* at 1 kV are secondaries which are not relevant to the modeling in this study. The *secondary peak* at 9 kV is not a recurrent phenomenon in the data and can be ignored. The *solid line* is a HYDRA particle flux which is approximately in conjunction with the FAST electron spectrum. The *dashed line* is the result of summing up two Maxwellian populations with densities of 0.25 and 0.29 $cm^{-3}$ and temperatures of 80 and 750 eV, respectively

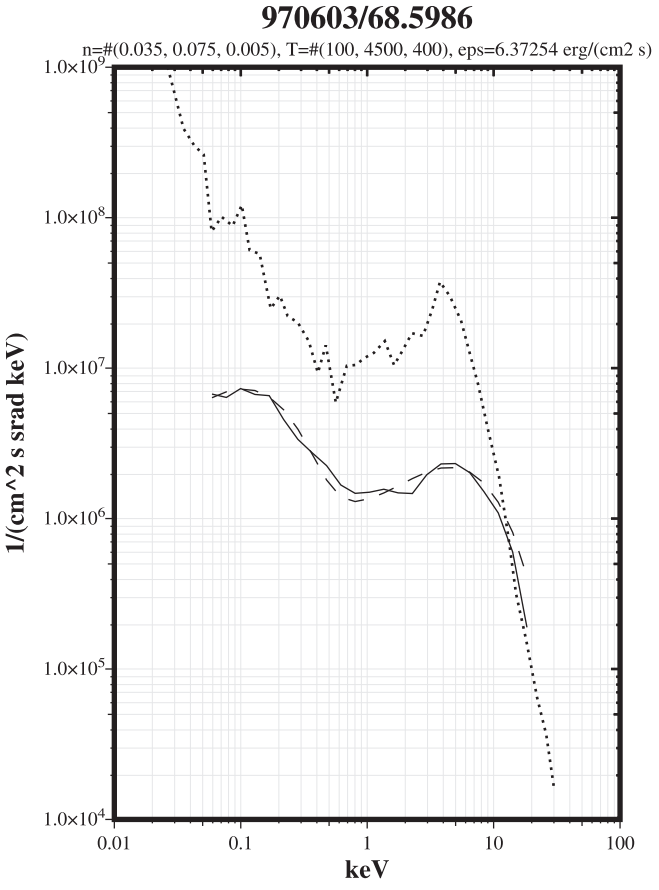


**Fig. 7.** Same as Fig. 6 but for the multiple-Maxwellian data example. The *dashed line* is the result of summing up three Maxwellian populations with densities 0.035, 0.075 and 0.005 $cm^{-3}$ and temperatures 100, 4500 and 400 eV, respectively

too narrow compared with the FAST electron spectrum. For energies higher than about 3 kV, however, it is in a pretty good agreement with FAST data.

One way to smear out the narrowness is to add random boosts as explained already, mimicing wave-particle interactions. When doing this, we run the SMU/randboost (Fig. 9). The agreement with data is now clearly better. The integrated energy flux is now 50% of the measurement, which is a modest improvement, but in the shape of the peak the improvement is bigger.

Let us now consider the O-shaped potential. In SMO/real (Fig. 10) the agreement with data is bad; however, the result is in agreement with the theoretical prediction (Table 2) as it should. Turning on random boosts (Fig. 11) with exactly the same parameters as were used in SMU/randboost, we get, interestingly, almost exactly the same result as from SMU/randboost. This is our most important finding from the simulation.

When boosts are included, the depth of the O-shaped potential and the U-shaped potential drop must be chosen to be slightly smaller than the wanted FAST peak position, because the boosts give the rest of the energy.

Since with random boosts, both U- and O-shaped potentials give a similar result, it is now interesting to see what happens if we turn off the electric field completely, i.e., just have the random parallel boosts. The result of this, SM/randboost, is shown in Fig. 12. The result in this case is actually not too far from real data (wave-particle interactions alone have also been suggested to explain auroral acceleration, Bryant and Perry, 1995), but anyway different enough from both SMU/randboost and SMO/randboost to show that the electric field structure is an important ingredient here. We will discuss this more thoroughly after presenting the runs for the multiple-Maxwellian case later.

We now turn to simulating the multiple-Maxwellian example, Fig. 7. Run MMU/real (Fig. 13) has the modeled source plasma and a U-shaped potential drop of magnitude 3.8 kV to match FAST peak position. The peak is now much too narrow and too high. The agreement in the energy flux (an integral over the peak) is rather good, about 60% of the measured value.

To make the peak more realistic we again include random boosts (Fig. 14). The agreement in the energy

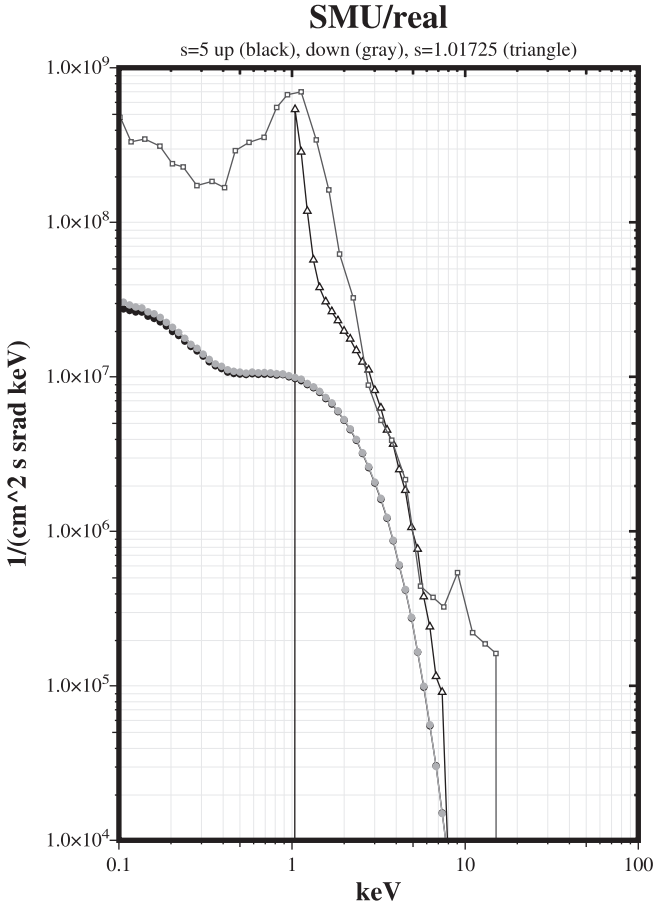


**Fig. 8.** SMU/real: source plasma corresponding to the *dashed line* in Fig. 6 accelerated through a U-shaped potential. The *line marked with squares* is the FAST data (the same as the *dotted line* in Fig. 6). The potential drop is selected to match FAST peak position (1.01 kV). The peak height is good but the peak is too narrow

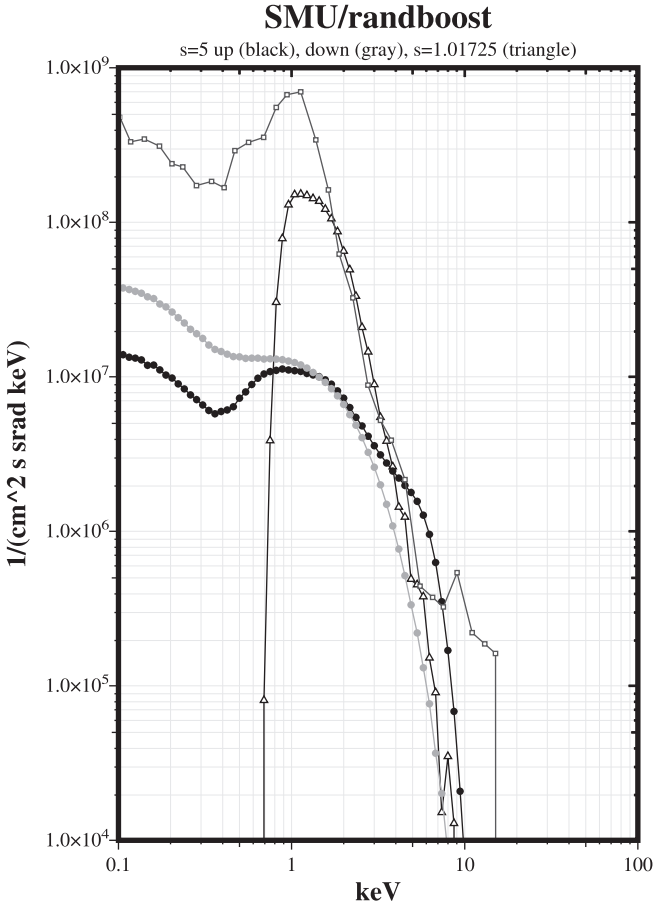


**Fig. 9.** SMU/randboost: same as model SMU/real (Fig. 8) but with random boosts added. The peak width is now better

flux is now very good (90% of the measured value), and also the shape of the peak is close to reality.

Going to the O-shaped potential, we first show the result without boosts (MMO/real, Fig. 15). Here the agreement is poor. But after including random boosts with the same parameters as in MMU/randboost we get essentially as good accordance with FAST data as with the U-shaped model. The result of MMO/randboost is shown in Fig. 16.

As was done in the SM example above, we now show the result without an electric field, i.e. only boosts remaining, in Fig. 17. The result shows that boosts alone are insufficient for producing a proper inverted-V peak in this case. The peak is more like a plateau.

As in the SM case, when boosts are included, the depth of the O-shaped potential and the U-shaped potential drop must be chosen to be slightly smaller than the wanted peak position, because the boosts give the rest of the energy. In the MM case the selected depth was 3 kV while the peak position was at 3.8 kV. This also means that the electrons which are just below the FAST peak but above the potential depth need not be secondaries: in the boosted case they are at least partly primary electrons.

## 3 Discussion and summary of simulation

We showed that the U- and O-shaped potentials behave in almost equivalent way if random parallel boosts are included in the altitude range which extends from the center of the O-shaped potentials about $2\,R_E$ upward. The might seem counterintuitive, since the O-shaped potential usually filters out some of the electrons and thus one could expect that the current and energy flux would always become smaller if an O-shaped potential is introduced. However, the simulation shows that this is not the case when boosts are included: the O- and U-shaped potentials produce almost identical low-altitude spectra, and if one removes the O-shaped potential (thus leaving just the boosts), the energy flux and current are *reduced*, not enhanced, and the good agreement with data is lost.

The physical explanation for this is as follows. The boost probability depends on the energy, thus when a low-energy particle is boosted a few times, it becomes a high-energy particle for which subsequent boosts may still happen but are very improbable. Thus, in the absence of an electric field, the effectiveness of boosts to increase the total energy flux is limited by the particles moving out (in energy space) from the efficient energy interval. In the upper half of an O-shaped potential, however, there is a downward electric field which tends

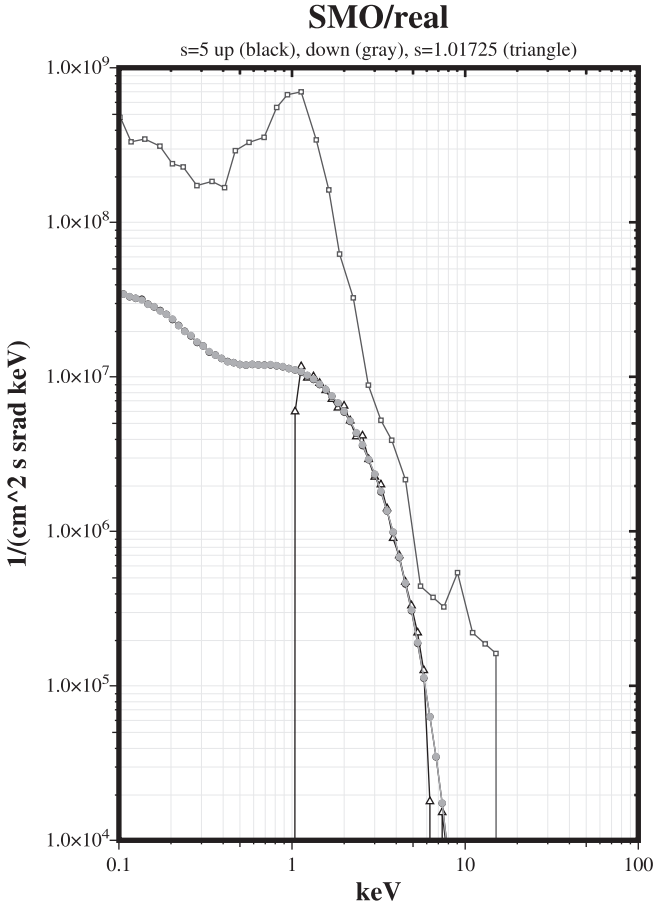


**Fig. 10.** SMO/real: same as model SMU (Fig. 4) but the particles now move through an O-shaped potential barrier instead of the U-shaped potential drop. The peak is much too low

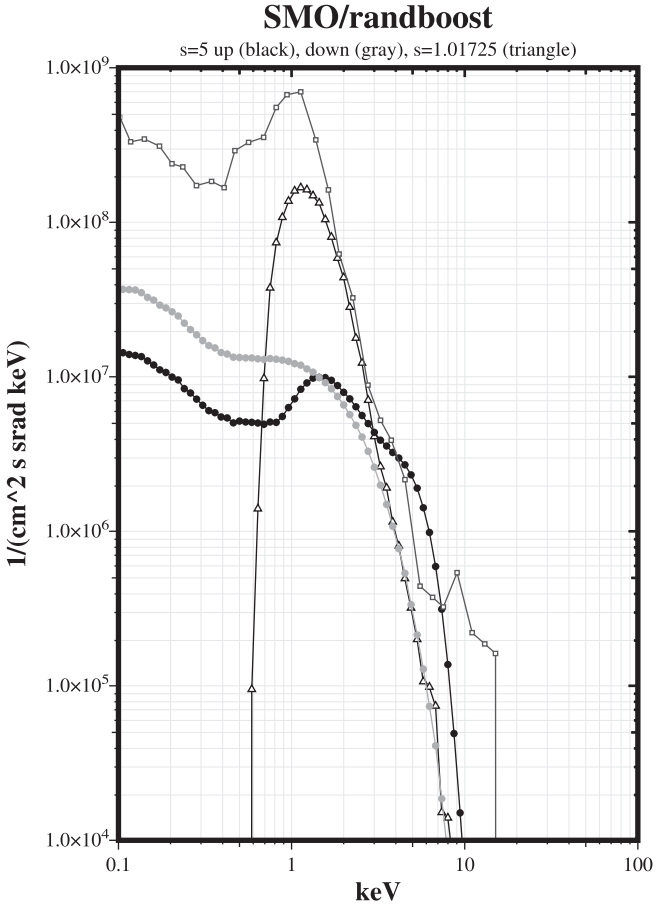


**Fig. 11.** SMO/randboost: same as model SMO/real (Fig. 10) but with random boosts included. The agreement is approximately as good as in SMU/randboost above (Fig. 9)

to push electrons upward (Fig. 1). Thus the boosts have to work against the potential, i.e., push the electrons up a potential "hill". This requires more energy (i.e., more energy is transferred to the electron population) because after being boosted downward, an electron slows down so it is more likely to be boosted again since it moves back towards the sensitive energy interval. In this way, the boosts can push a lot of electrons up the hill, and the lower part of the O-shaped potential gives them the final acceleration and produces the inverted-V peak in the correct position.

The electron acceleration mechanism may modify the distribution function at the upper boundary ($s = 5$) also, especially if it is caused by wave-particle interactions which are symmetric with respect to up and downgoing particles. This is seen in our results as a difference between the black and gray dotted curves (up and downgoing populations at $s = 5$). The downgoing populations at $s = 5$ is fixed to the prescribed distribution function by the boundary condition, but the upgoing part has been modified by the acceleration processes. The presence of a simulation box boundary at $s = 5$ most probably overestimates the difference between the up and downgoing populations relative to the real magnetosphere where no such boundary exists.

The shaded area in Fig. 18 shows those electrons that are just below the main peak and which are usually explained as being backscattered primaries which have degraded in energy (Evans, 1974). The random parallel boosts produce particles in this range also directly. Thus with a model containing the boosts, this region of the spectrum can be partly composed of primaries that have not interacted with the ionosphere.

Let us discuss the energetics of the MM/randboost case (Fig. 17). The observed electron precipitation amounts to $6.4\,\mathrm{mW\,m^{-2}}$ (Table 2), which means that to power the aurora below, about $0.06\,\mathrm{mW\,m^{-2}}$ must be entered through the upper end of the simulation box (the value 6.4 multiplied by roughly 0.01, the ratio of flux tube areas at the ionosphere and at $4\,R_E$ altitude). This can occur either by waves as a Poynting flux, or by particles. A Poynting flux of $0.06\,\mathrm{mW\,m^{-2}}$ could be produced by waves having (e.g.) 70 mV/m electric amplitude and 1 nT magnetic component. Considering particles, the hot electron population temperature is 4.5 keV and partial density $0.075\,\mathrm{cm^{-3}}$, which yields $1.21\,\mathrm{mW\,m^{-2}}$ energy flux. This is 20 times larger than the required flux $0.06\,\mathrm{mW\,m^{-2}}$. In other words, if the hot electrons carry the energy, they would have to experience a reduction in energy of only 5% during each

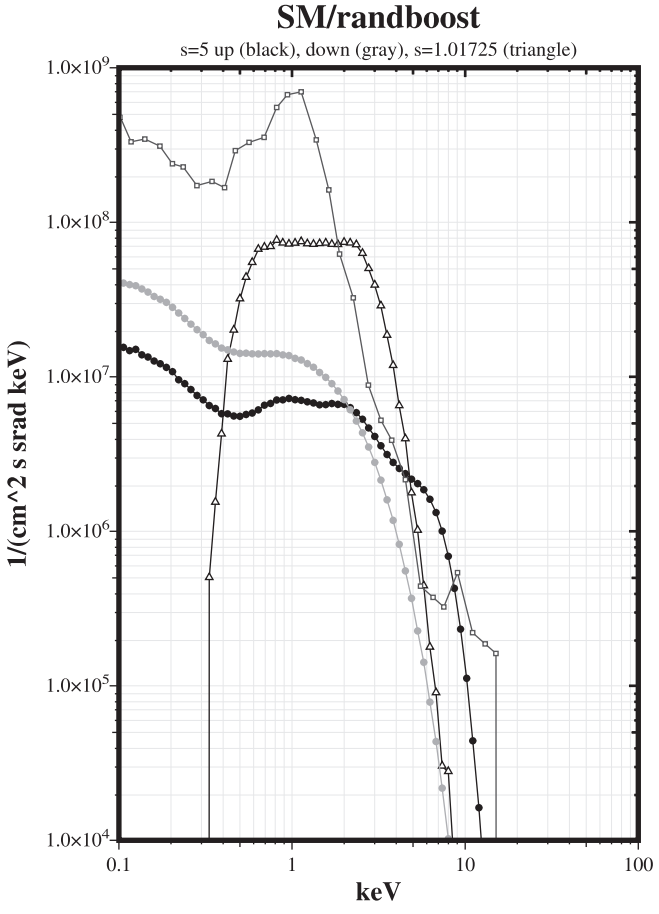


**Fig. 12.** SM/randboost: same as SMO/randboost but without electric field (only boosts left). The peak looks rather unrealistic now

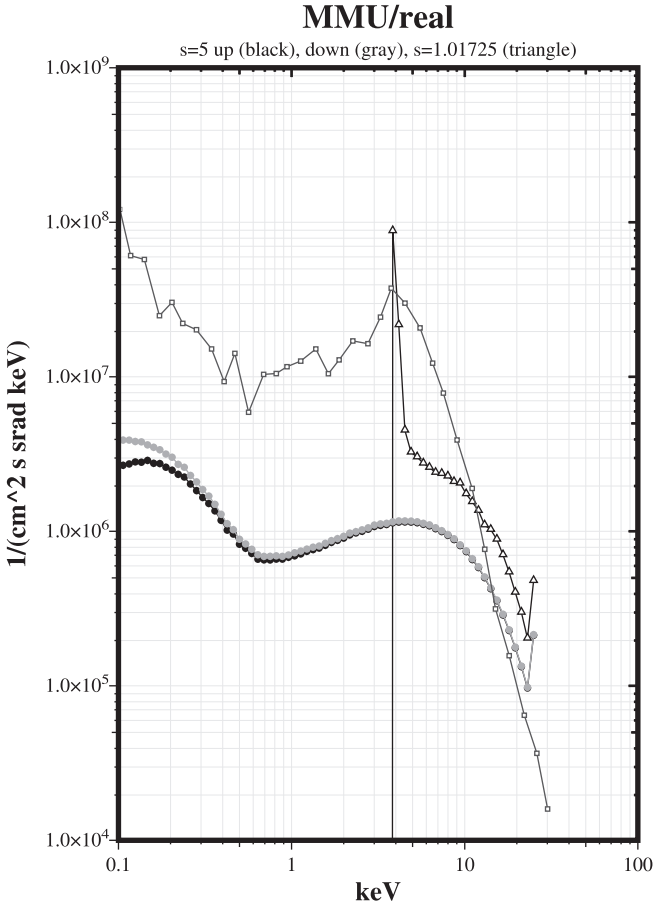


**Fig. 13.** MMU/real: source plasma corresponding to the *dashed line* in Fig. 7 accelerated through a U-shaped potential. The *line marked with squares* is the FAST data (the same as the *dotted line* in Fig. 7). The potential drop is selected to match FAST peak position (3.8 kV). The peak is much too narrow and its shape is unnatural

bounce below $4\,R_E$ altitude level. Such a small change would be hard to detect. The energy flux of hot ions is probably roughly similar in magnitude, even though we cannot compute it exactly based on out measurements because the hot ions are partly beyond HYDRA maximum energy.

It is important to note that even though waves are assumed in our model to play a crucial role in creating the loss cone population, it is still quite possible that hot particles, not waves, carry the energy through the upper end of the flux tube at $4\,R_E$ altitude. This can be so e.g., if waves do not propagate long distances but are created and damped at approximately the same altitude. Even purely electric waves, whose Poynting flux is by definition zero (no magnetic component in the wave), could in principle accomplish the required pitch angle scattering in out model.

We have kept the random parallel boost model as simple as possible, for example, the boosting process is limited to a fixed altitude range ($2.5 \leq s \leq 4.25$ in most cases), and the process is similar throughout the range. While a model that contained more parameters might correspond to data even better, we think that until we have a specific physical wave-particle interaction to account for by the boosting process, such refinements would be premature.

We summarize the findings from the test particle simulations.

1. The results of the simulation model are in quantitative agreement with analytic theory in cases where analytic theory is applicable (adiabatic motion).
2. A U-shaped potential drop gives a total energy flux of the correct order of magnitude, but the peak becomes too narrow (SMU, MMU). In the SMU case the discrepancy is not very striking, but in the MMU case it is.
3. The peak looks more realistic if random boosts are included (SMU/randboost, MMU/randboost).
4. When using random boosts, the U-shaped potential drop can be replaced by an O-shaped potential barrier without much affecting the results (SMO/randboost, MMO/randboost). But this does not mean that the electric field is irrelevant, since without it (SM/randboost, MM/randboost) the results is completely different, especially in the MM case.
5. When boosts are there, inserting an O-shaped potential barrier *increases* the energy flux and current.
6. The explanation for the previous two points is that when boosts work against an electrostatic force, the

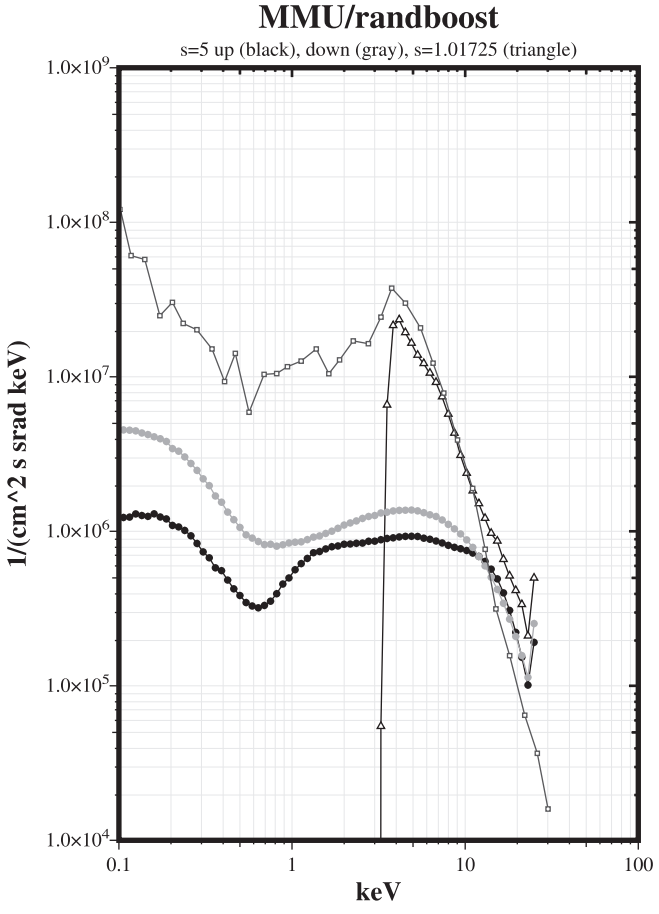


**Fig. 14.** MMU/randboost: same as model MMU/real (Fig. 13) but with random boosts added. The agreement is pretty good

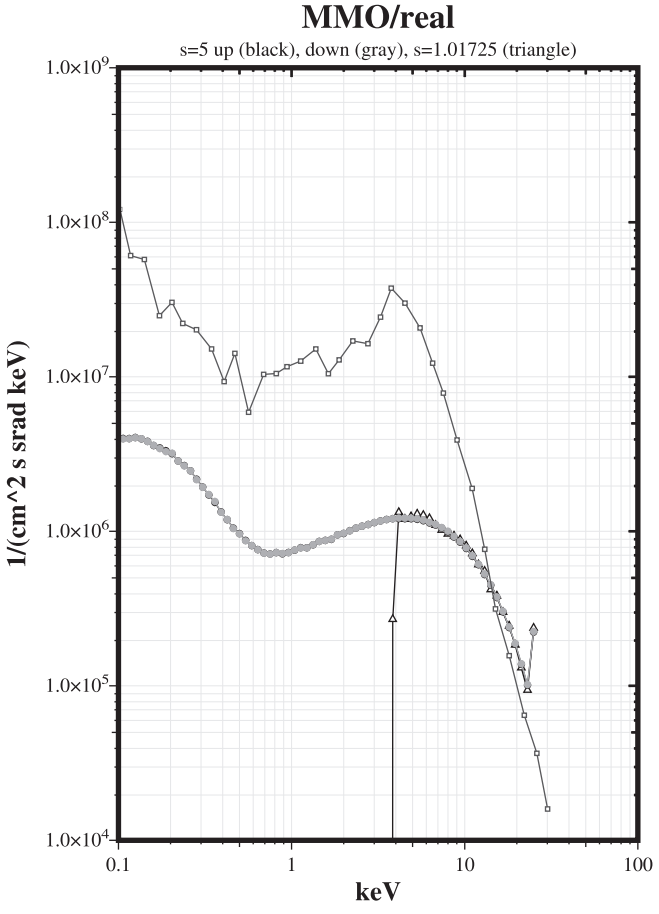


**Fig. 15.** MMO/real: same as model MMU (Fig. 13) but the particles now move through an O-shaped potential barrier instead of the U-shaped potential drop. The peak is too low

amount of total energy transferred to the electrons can be larger than without the electric field. We call this the "hill" effect. Thus, realistic inverted-V spectra can be produced by a model which includes an O-shaped potential and random parallel boosts in cooperation, even though each one taken alone produces a result that is far from being realistic.

## 4 The "cooperative" model

Based on these findings, we suggest that the following model might explain those inverted-V events where the U-shaped model is not applicable (Fig. 19).

The potential geometry is O-shaped. The lower part of the potential (which is U-shaped) contains a similar acceleration region as in the U-shaped model, i.e., the electrons are accelerated towards the ionosphere by a quasistatic potential drop. Most of the low-altitude phenomenology is therefore the same as in the U-shaped model. Above the center of the "O" the quasistatic electric field points downward. In this region there are plasma waves which accelerate low- and middle-energy electrons in the parallel direction, thus forcing them inside the loss cone. It helps if the acceleration is predominantly downward, but a symmetric acceleration, as was assumed in the calculation presented here, will also do. The point is that since the waves are pushing the electrons up a potential hill, they remain in the resonant velocity interval for a longer time. Therefore the waves do not accelerate the electrons to very high speeds, but only modify the pitch angle distribution of low- and middle-energy populations so that more electrons are found in the loss cone. Thus this region can be called the *auroral energization region*, since electrons gain potential energy, but not so much kinetic energy, from the waves. The gained potential energy is turned into kinetic energy further below, in the usual acceleration region.

To maintain the O-shaped potential structure requires a net negative charge cloud in the center of the "O". This charge cloud can be provided self-consistently by the anisotropic pitch angle distribution of the electrons: since $T_{\parallel} > T_{\perp}$, the mirror points move towards the ionospheric (Alfvén and Fälthammar, 1963), producing a negative charge cloud which becomes stronger as one moves downward. At and close to the ionosphere the charge cloud is easily neutralized by ionospheric particles because of the flux tube convergence, thus the charge cloud will have a maximum at some altitude, which becomes the altitude of the center of the O-shaped potential.

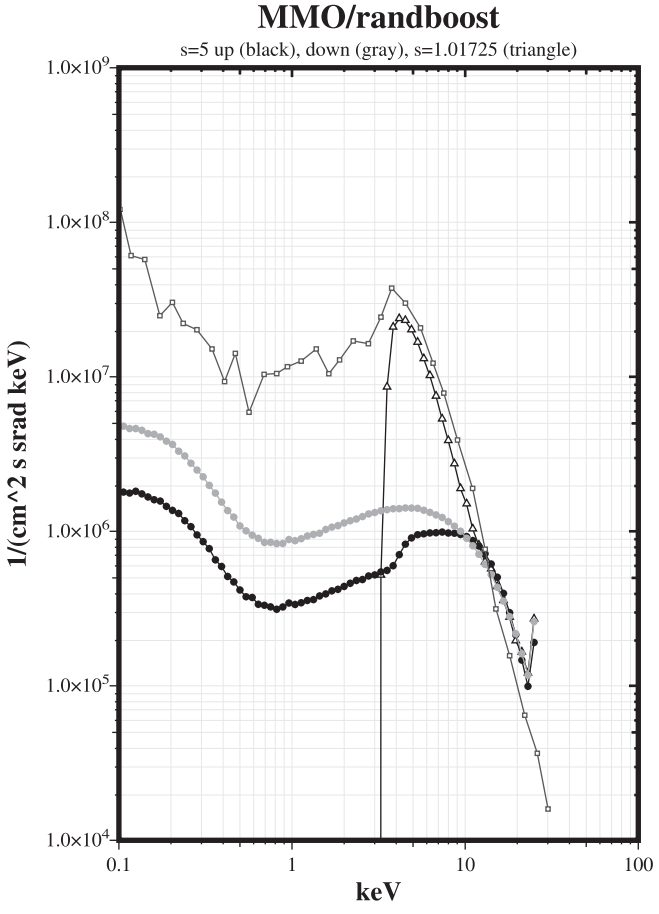


**Fig. 16.** MMO/randboost: same as model MMO/real (Fig. 15) but with random boosts included. The agreement is good

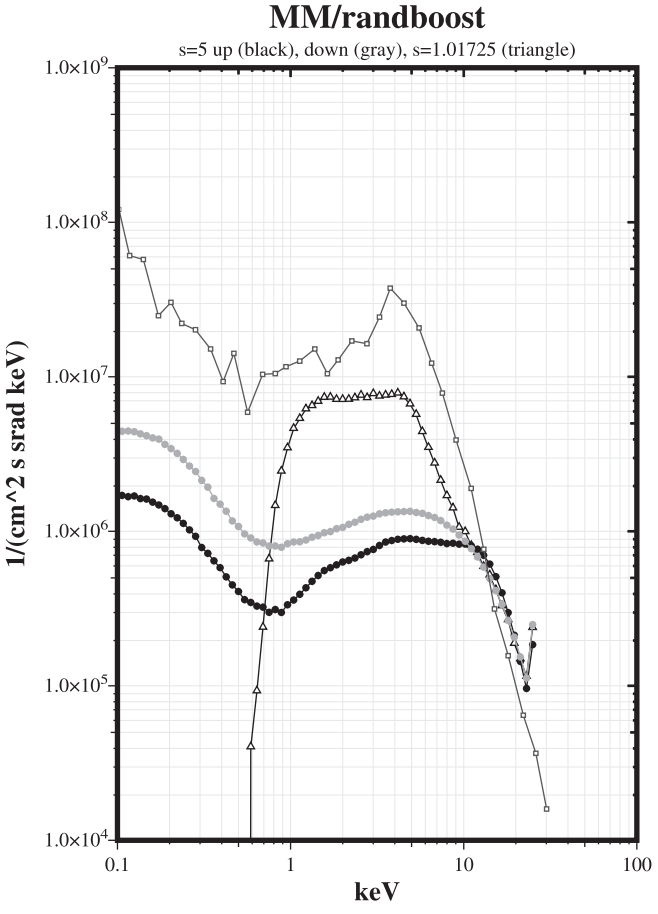


**Fig. 17.** MM/randboost: same as MMO/randboost but without electric field (only boosts left). The result looks quite unrealistic

Let us consider in qualitative terms how the auroral plasma responds to a primary charge cloud. The electrons are the first to respond. Quasineutrality must be preserved, so a parallel electrostatic field is set up which displaces the pre-existing electrons in such a way as to make the total electron density equal to the ion density, which remains stationary in the electron time scale. The plasma consists of a cold component of ionospheric origin, the density of which rapidly falls with increasing height, and a magnetospheric hot component, whose density is almost constant. At a given altitude, if the primary cloud density is smaller than the cold electron density, a small negative potential with magnitude of the order of the cold electron thermal energy (tens of eV at most) is sufficient to displace the required amount of cold electrons from the region. If the primary cloud density is larger than the cold electron density, however, also some of the hot electrons must be displaced, which requires that a much larger potential develops. The magnitude of the potential must now be of the order of the hot electron thermal energy. The resulting combined potential is a negative potential barrier (O-shaped potential) whose lower limits is sharp and resides at the altitude where the cold plasma density is equal to the primary charge cloud density. Here the electric field points upward. The upper part of the potential well is smoothly varying and has a downward

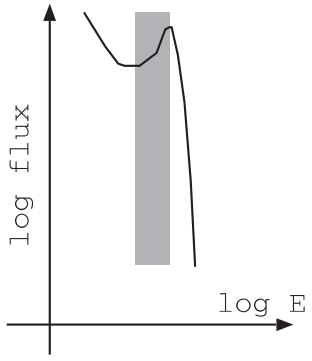


**Fig. 18.** The portion of electrons which is conventionally in the U-shaped potential drop model explained as backscattered and degraded primaries, can in the "boosted" O-shaped potential barrier model be produced by the wave-particle interactions directly

electric field. Thus the electrons respond in such a way that an asymmetric potential well is set up whose depth is of the order of the hot magnetospheric electron temperature.

The ions respond much slower than the electrons. The potential well attracts the ions, but since energy is conserved, they just move through the well with an increased speed. The ions can start to annihilate (neutralize) the potential well only if they lose energy

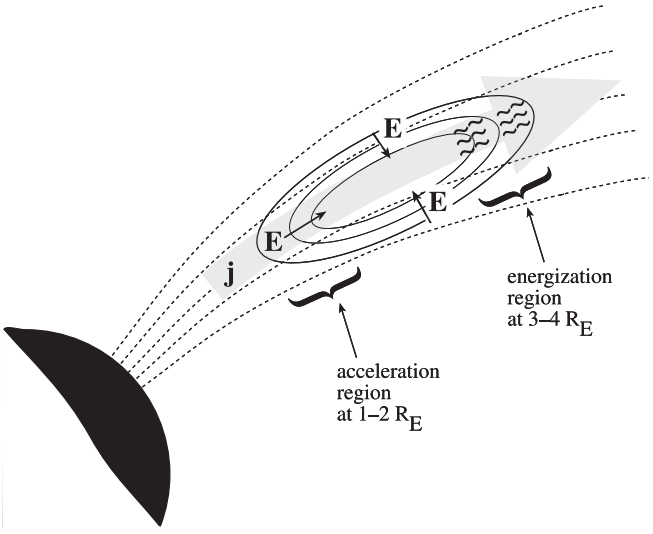


**Fig. 19.** "Cooperative" model for auroral arc acceleration: the energy is provided by plasma waves in the "energization region", but the agent for acceleration is a static electric field in the acceleration region. The O-shaped potential structure is maintained by the anisotropic pitch angle distribution caused by the waves. Upward electric current carried by the precipitating electrons is indicated by *gray arrow*

while passing through the structure by some anomalous processes and thus become trapped by the well.

Considering energy transfer, the primary reason for the auroral acceleration process in this model is the existence of plasma waves in the energization region, which accelerate the electrons and increase the parallel energy. The waves could be, for example, the lower-hybrid waves proposed earlier (Bingham *et al*., 1988, 1991), or any waves having a parallel phase velocity close to the parallel thermal speed of some of the cooler electrons, numerically about 2000–6000 km/s. The parallel energy increase of the electrons gives rise to a charge cloud, which, after becoming partly neutralized by ionospheric ions, becomes an O-shaped potential. The downward electric field associated with the potential structure helps extract more energy from the waves by keeping the electrons in the resonant velocity range for a longer time. The lower part of the system has an electrostatic acceleration region exactly in the same way as in the U-shaped model. The O-shaped structure as a whole acts as an intermediate potential energy storage, which enables the acceleration region to reside below the energization region.

In summary, the "cooperative model" is self-consistent and compatible with the observed absence of convergent electric fields at $4\,R_E$, without contradicting the well-established low-altitude phenomenology. An observational validation of the model would require quantitative observations of the required waves in the energization region (roughly 3–4 $R_E$ altitude range). In any case, the new model presents us with a significantly modified picture of the energy flow mechanisms that can be responsible for creating and maintaining auroral arcs and inverted-V acceleration regions.

*Acknowledgements*. The authors thank Craig A. Kletzing and James P. McFadden for providing HYDRA and FAST data for the example, and Harri Laakso, Rolf Boström, Anders Eriksson and Kirsti Kauristie for many useful discussions, encouragement and practical help. We also thank both referees for valuable and constructive comments.

Topical Editor G. Chanteer thanks H. de Féraudy and another referee for their help in evaluating this paper.

## References

**Alfvén, H., and C. G. Fälthammar,** *Cosmical electrodynamics*, Clarendon, Oxford 1963.

**Bingham, R., D. A. Bryant, and D. S. Hall,** Auroral electron acceleration by lower-hybrid waves, *Ann. Geophysicae*, **6,** 159–168, 1988.

**Bryant, D. A.,** *Electron acceleration in the aurora and beyond*, Institute of Physics Publishing, Bristol, 1999.

**Bryant, D. A., and C. H. Perry,** Velocity-space distributions of wave-accelerated auroral electrons, *J. Geophys. Res.*, **100,** 23 711–23 725, 1995.

**Bryant, D. A., A. C. Cook, Z.-S. Wang, U. De Angelis, and C. H. Perry,** Turbulent acceleration of auroral electrons, *J. Geophys. Res.*, **96,** 13 829–13 839, 1991.

**Carlqvist, P., and R. Boström,** Space-charge regions above the aurora, *J. Geophys. Res.*, **75,** 7140–7146, 1970.

**Evans, D. S.,** Precipitating electron fluxes formed by a magnetic field aligned-potential difference, *J. Geophys. Res.*, **79,** 2853–2858, 1974.

**Fridman, M., and J. Lemaire,** Relationship between auroral electron fluxes and field aligned electric potential differences, *J. Geophys. Res.* **85,** 664–670, 1980.

**Janhunen, P., and A. Olsson,** The current-voltage relationship revisited: exact and approximate formulas with almost general validity for hot magnetospheric electrons for bi-Maxwellian and kappa distributions, *Ann. Geophysicae*, **16,** 292–297, 1998.

**Janhunen, P., A. Olsson, F. S. Mozer, and H. Laakso,** How does the U-shaped potential close above the acceleration region? A study using Polar data, *Ann. Geophysicae*, **17,** 1276–1283, 1999.

**Lin, C. S, and R. A. Hoffman,** Characteristics of the inverted-V event, *J. Geophys. Res.*, **84,** 1514–1525, 1979.

**Marklund, G.,** Viking investigations of auroral electrodynamical processes, *J. Geophys. Res.*, **98,** 1691–1704, 1993.

**McFadden, J. P., C. W. Carlson, R. E. Ergun, F. S. Mozer, M. Temerin, W. Peria, D. M. Klumpar, E. G. Shelley, W. K. Peterson, E. Moebius, L. Kistler, R. Elphic, R. Strangeway, C. Cattell, and R. Pfaff,** Spatial structure and gradients of ion beams observed by FAST, *Geophys. Res. Lett.*, **25,** 2021–2024, 1998.

**Shelley, E. G., and H. L. Collin,** Auroral ion acceleration and its relationship to ion composition, in *Auroral physics*, Eds. Meng, Rycroft and Frank, Cambridge University Press, 1991.